International Journal of Bifurcation and Chaos, Vol. 23, No. 3 (2013) 1350057 (17 pages)

DOI: 10.1142/S0218127413500570

BIFURCATIONS AND EXACT TRAVELING WAVE SOLUTIONS FOR A GENERALIZED CAMASSA–HOLM EQUATION*

JIBIN LI
Department of Mathematics,
Zhejiang Normal University, Jinhua,
Zhejiang 321004, P. R. China
lijb@zjnu.cn
jibinli@gmail.com

ZHIJUN QIAO
Department of Mathematics,
The University of Texas Pan-American,
1201 West University Drive,
Edinburg, TX 78541, USA

Received September 5, 2012; Revised November 10, 2012

In this paper, we study all possible traveling wave solutions of an integrable system with both quadratic and cubic nonlinearities: $m_t = bu_x + \frac{1}{2}k_1[m(u^2 - u_x^2)]_x + \frac{1}{2}k_2(2mu_x + m_x u)$, $m = u - u_{xx}$, where b, k_1 and k_2 are arbitrary constants. We call this model a generalized Camassa–Holm equation since it is kind of a cubic generalization of the Camassa–Holm (CH) equation: $m_t + m_x u + 2mu_x = 0$. In the paper, we show that the traveling wave system of this generalized Camassa–Holm equation is actually a singular dynamical system of the second class. We apply the method of dynamical systems to analyze the dynamical behavior of the traveling wave solutions and their bifurcations depending on the parameters of the system. Some exact solutions such as smooth soliton solutions, kink and anti-kink wave solutions, M-shape and W-shape wave profiles of the breaking wave solutions are obtained. To guarantee the existence of those solutions, some constraint parameter conditions are given.

Keywords: Generalized Camassa–Holm equation; soliton solution; kink and anti-kink wave solutions; breaking wave solution; bifurcation.

1. Introduction

The Camassa–Holm (CH) equation

$$m_t - bu_x + 2mu_x + m_x u = 0, \quad m = u - u_{xx}, \quad (1)$$

was derived in [Camassa & Holm, 1993] as a shallow water wave model. In recent years, this equation has attracted much attention in the studies of soliton theory. In the literature, this equation was derived from [Fuchssteiner & Fokas, 1981] on hereditary symmetries as a very special case. However, since the work of [Camassa *et al.*, 1994], various studies on this equation have been developed. The CH equation possesses many important integrable properties. For instance, it admits the Lax

*The authors are supported by the National Natural Science Foundation of China (10831003).

representation, bi-Hamiltonian structures, multi-soliton solutions, and algebraic-geometric solutions (see [Camassa *et al.*, 1994; Olver & Rosenau, 1996]). Also, it is integrable by the inverse scattering transformation [Constantin *et al.*, 2007]. The most remarkable feature of the CH equation is having peaked soliton (peakon) solutions in the case of $b = 0$. A peakon is a weak solution in some Sobolev space with corner at its crest.

In addition to the CH equation being an integrable model that admits the peakon solutions, other integrable peakon models have been found. Those integrable peakon models include the Degasperis–Procesi equation, among others (see [Li & Chen, 2007; Li & Dai, 2007; Li *et al.*, 2006; Li & Qiao, 2010] and cited references therein).

The present paper focuses on the following equation with both quadratic and cubic nonlinearities:

$$m_t = bu_x + \frac{1}{2}k_1[m(u^2 - u_x^2)]_x + \frac{1}{2}k_2(2mu_x + m_x u), \quad m = u - u_{xx}, \tag{2}$$

where b, k_1 and k_2 are three arbitrary constants. It is clear that Eq. (2) reduces to the CH equation (1) when $k_1 = 0$, $k_2 = -2$. For $k_1 = -2$, $k_2 = 0$, Eq. (2) is exactly the cubic nonlinear equation:

$$m_t - bu_x + [m(u^2 - u_x^2)]_x = 0, \quad m = u - u_{xx}, \tag{3}$$

which was derived independently by Fokas [1995], Fuchssteiner [1996], Olver and Rosenau [1996], Qiao [2006], where the equation was derived from the two-dimensional Euler system, for which the Lax pair, the M/W-shape solitons and cuspon solutions were presented in [Qiao, 2006, 2007; Qiao & Li, 2011].

Equation (2) is actually a linear combination of the CH equation (1) and cubic nonlinear equation (3). Therefore, we may view Eq. (2) as a generalization of the CH equation, so we simply call it a generalized CH equation. This structure is very similar to the one in dealing with the Gardner equation, known as a linear combination of the KdV and mKdV equations, which has important applications in various areas of physics (see [Desanto, 1998]). In fact, the structure of the Gardner equation is our starting point to study Eq. (2). We also notice that by some appropriate rescaling, Eq. (2) might implicitly be derived from [Fokas, 1995; Fuchssteiner, 1996] in the context of hereditary symmetries.

In this paper, we study the dynamical behavior of all traveling wave solutions of (2) and our objective is to find possible exact parametric representations of the bounded traveling wave solutions of (2). For this purpose, let $u(x,t) = \phi(x - ct) = \phi(\xi)$, where c is the wave speed. Substituting it into Eq. (2), integrating the obtained equation once and setting the integration constant as 0, we have

$$\phi''\left(c + \frac{1}{2}k_2\phi + \frac{1}{2}k_1\phi^2 - \frac{1}{2}k_1(\phi')^2\right) = \left((b+c)\phi + \frac{3}{4}k_2\phi^2 + \frac{1}{2}k_1\phi^3\right) - \left(\frac{1}{4}k_2 + \frac{1}{2}k_1\phi\right)(\phi')^2, \tag{4}$$

where "$'$" stands for the derivative with respect to ξ.

Equation (4) is equivalent to the following two-dimensional system:

$$\frac{d\phi}{d\xi} = y, \quad \frac{dy}{d\xi} = \frac{-\left(\frac{1}{4}k_2 + \frac{1}{2}k_1\phi\right)y^2 + \phi\left((b+c) + \frac{3}{4}k_2\phi + \frac{1}{2}k_1\phi^2\right)}{c + \frac{1}{2}k_2\phi + \frac{1}{2}k_1\phi^2 - \frac{1}{2}k_1 y^2}, \tag{5}$$

which has the first integral

$$H(\phi, y) = \frac{1}{2}y^2\left(c + \frac{1}{2}k_2\phi + \frac{1}{2}k_1\phi^2\right) - \frac{1}{8}k_1 y^4 - \left((b+c)\phi^2 + \frac{1}{4}k_2\phi^3 + \frac{1}{8}k_1\phi^4\right) = h. \tag{6}$$

Without loss of generality, we assume that the wave speed c (> 0) is given. Then, system (5) is a three-parameter planar dynamical system depending on the parameter group (b, k_1, k_2). We attempt to investigate all possible phase portraits of (5) in the phase plane (ϕ, y) when the parameter group (b, k_1, k_2) is varied. We only discuss the bounded solutions of system (5).

Notice that for $k_1 \neq 0$, the right-hand side of the second equation of (5) is not continuous on the hyperbola $c + \frac{1}{2}k_2\phi + \frac{1}{2}k_1\phi^2 - \frac{1}{2}k_1y^2 = 0$, i.e. $(\phi + \frac{k_2}{2k_1})^2 - y^2 = \frac{k_2^2-8k_1c}{4k_1^2} \equiv R$. In fact, along this curve in the phase plane (ϕ, y), ϕ''_ξ is not well defined. Therefore, this class of systems is called the second class of singular traveling wave systems by [Li *et al.*, 2010].

This paper is organized as follows. In Sec. 2, we discuss the bifurcations of phase portraits of system (5) under different parameter conditions. In Sec. 3, we find all explicit parametric representations for solitary wave solutions, kink wave solutions, M-shape type and W-shape type breaking wave solutions as well as two-peak wave solutions of Eq. (3), when the phase portraits of (5) are symmetric. In Sec. 4, as an example, we derive the explicit parametric representations of the M-shape type of breaking wave solutions of Eq. (2), when the phase portraits of (5) are nonsymmetric.

2. Bifurcations of Phase Portraits of (5)

We assume that $c > 0, k_1 \neq 0$. Imposing the transformation $d\xi = (c + \frac{1}{2}k_2\phi + \frac{1}{2}k_1\phi^2 - \frac{1}{2}k_1y^2)d\zeta$ for $c + \frac{1}{2}k_2\phi + \frac{1}{2}k_1\phi^2 - \frac{1}{2}k_1y^2 \neq 0$ on system (5) leads to the following cubic system:

$$\begin{aligned}\frac{d\phi}{d\zeta} &= y\left(c + \frac{1}{2}k_2\phi + \frac{1}{2}k_1\phi^2 - \frac{1}{2}k_1y^2\right),\\ \frac{dy}{d\zeta} &= -\left(\frac{1}{4}k_2 + \frac{1}{2}k_1\phi\right)y^2\\ &\quad + \phi\left((b+c) + \frac{3}{4}k_2\phi + \frac{1}{2}k_1\phi^2\right).\end{aligned} \tag{7}$$

Making the transformation $\phi = \varphi - \frac{k_2}{2k_1}, \eta = \frac{k_1}{2}\zeta$, systems (5) and (7) become respectively the following:

$$\begin{aligned}\frac{d\varphi}{d\xi} &= y,\\ \frac{dy}{d\xi} &= \frac{-\varphi y^2 + \varphi^3 + A\varphi + B}{(\varphi^2 - y^2 - R)}\end{aligned} \tag{5$_\mathrm{a}$}$$

and

$$\begin{aligned}\frac{d\varphi}{d\eta} &= y(\varphi^2 - y^2 - R),\\ \frac{dy}{d\eta} &= -\varphi y^2 + \varphi^3 + A\varphi + B\\ &= -\varphi y^2 + \left(\varphi - \frac{k_2}{2k_1}\right)\\ &\quad \times \left(\varphi^2 + \frac{k_2}{2k_1}\varphi + \frac{4k_1(b+c) - k_2^2}{2k_1^2}\right),\end{aligned} \tag{8}$$

where $A = \frac{8k_1(b+c)-3k_2^2}{4k_1^2}, B = \frac{k_2(k_2^2-4k_1(b+c))}{4k_1^3}, R = \frac{k_2^2-8k_1c}{4k_1^2}$. Correspondingly, the first integral (6) becomes

$$\begin{aligned}H_1(\varphi, y) &= -\frac{1}{4}(\varphi^2 - y^2)^2\\ &\quad - \frac{1}{2}A\varphi^2 - \frac{1}{2}Ry^2 - B\varphi = h.\end{aligned} \tag{9}$$

Thus, we have

$$\begin{aligned}y^2 &= (\varphi^2 - R)\\ &\quad \pm \sqrt{(R^2 - 4h) - 4B\varphi - 2(A+R)\varphi^2}.\end{aligned} \tag{10}$$

We now consider the equilibrium points of (8). Write $\Delta = 9k_2^2 - 32k_1(b+c)$. Clearly, when $\Delta > 0$, in the φ-axis, Eq. (8) has three equilibrium points $E_0(\varphi_0, 0), E_{1,2}(\varphi_{1,2}, 0)$, where $\varphi_0 = \frac{k_2}{2k_1}, \varphi_{1,2} = \frac{1}{4k_1}[-k_2 \mp \sqrt{\Delta}]$. When $\Delta_1 = k_2^2(c-2b) + 8k_1b^2 > 0$ and $k_2^2 - 4bk_1 \neq 0$, on the hyperbola $\varphi^2 - y^2 = R$, (8) has two equilibrium points $S_{1,2}(\varphi_s, Y_\pm)$, where $\varphi_s = \frac{k_2[k_2^2-4k_1(b+c)]}{2k_1[k_2^2-4bk_1]}, Y_\pm = \pm\frac{2\sqrt{c\Delta_1}}{|k_2^2-4bk_1|}$.

Let $M(\varphi_j, 0)$ be the coefficient matrix of the linearized system of (6) at an equilibrium point $E_j(\varphi_j, 0)$. We have

$$\begin{aligned}J(\varphi_j, 0) &= \det M(\varphi_j, 0)\\ &= (R - \varphi_j^2)(3\varphi_j^2 + A).\\ J(\varphi_s, Y_\pm) &= \det M(\varphi_s, Y_\pm)\\ &= 2Y_\pm^2[\varphi_s^2 - 2\varphi_s + 2R + A].\end{aligned}$$

By the theory of planar dynamical systems, for an equilibrium point of a planar integrable system, if $J < 0$, then the equilibrium point is a saddle point; if $J > 0$, then it is a center point; if $J = 0$ and the Poincaré index of the equilibrium point is 0, then this equilibrium point is a cusp (see [Li & Dai, 2007]).

For notational convenience, denote

$$h_0 = H_1(\varphi_0, 0) = \frac{k_2^2}{64k_1^4}[-3k_2^2 + 16k_1(b+c)],$$

$$h_1 = H_1(\varphi_1, 0) = \frac{\varphi_1}{64k_1^3}[-15k_2^3 + 56k_1k_2(b+c) + (8k_1(b+c) - 3k_2^2)\sqrt{\Delta}],$$

$$h_2 = H_1(\varphi_2, 0) = \frac{\varphi_2}{64k_1^3}[15k_2^3 - 56k_1k_2(b+c) + (8k_1(b+c) - 3k_2^2)\sqrt{\Delta}],$$

$$h_s = H_1(\varphi_s, Y_\pm) = \frac{3k_2^6 - 4k_2^4k_1(7b+4c) + 64k_1^2k_2^2b(b+c) + 256k_1^3bc^2}{64k_1^4(4k_1b - k_2^2)}.$$

1. *The case of* $B = \frac{k_2(k_2^2 - 4k_1(b+c))}{4k_1^3} = 0$. Under this parametric condition, the phase portraits of (8) are symmetric.

(i) $k_1 \neq 0, k_2^2 = 4k_1(b+c) \geq 0$.

In this case, we have that $A = -\frac{b+c}{k_1}$, $\Delta = 4k_1(b+c)$, $\Delta_1 = 4k_1c(c-b)$, $R = \frac{b-c}{k_1}$, $\varphi_1 = -\frac{\sqrt{k_1(b+c)}}{k_1} = -\frac{k_2}{2k_1}$, $\varphi_2 = 0$, $\varphi_s = 0$, $Y_\pm = \pm\frac{\sqrt{-k_1(b-c)}}{|k_1|}$, $h_1 = \frac{(b+c)^2}{4k_1^2} = h_0$, $h_2 = 0$, $h_s = \frac{(b-c)^2}{4k_1^2}$.

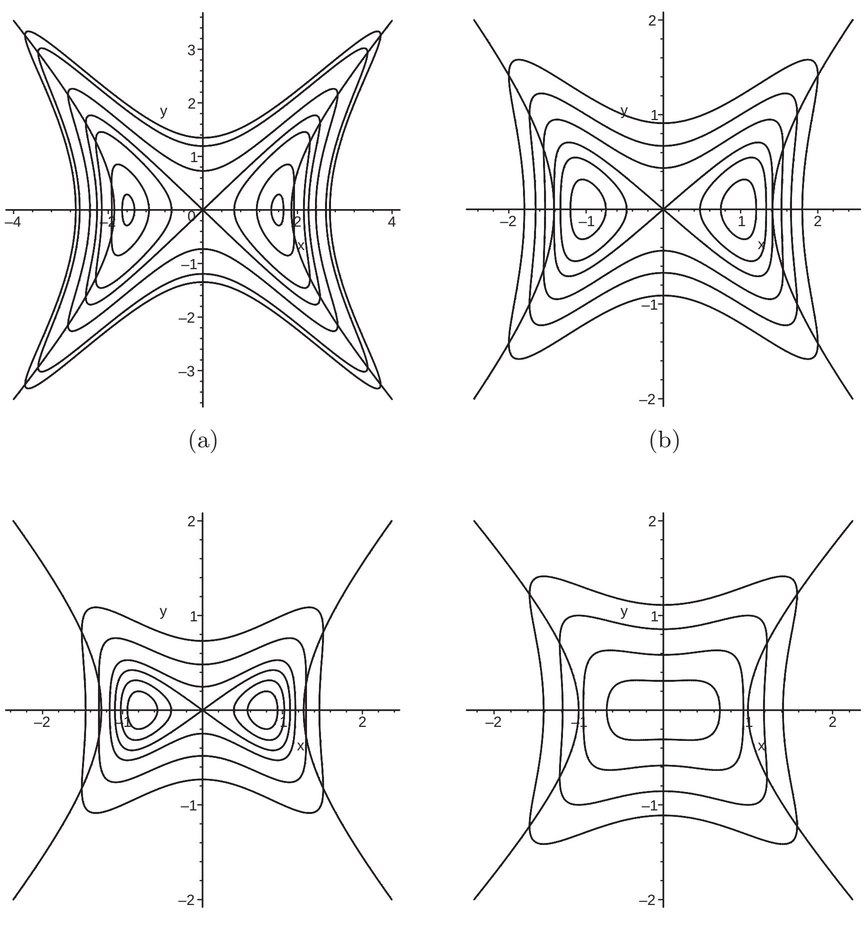

Fig. 1. The bifurcations of phase portraits of system (11) for $k_1 < 0, b+c \leq 0$. (a) $-\infty < b < -3c$, (b) $b = -3c$, (c) $-3c < b < -c$ and (d) $b = -c$.

System (8) becomes

$$\frac{d\varphi}{d\eta} = y\left(\frac{c-b}{k_1} + \varphi^2 - y^2\right), \quad \frac{dy}{d\eta} = -\varphi\left(\frac{b+c}{k_1} - \varphi^2 + y^2\right). \tag{11}$$

For $k_1 < 0$ and $k_1 > 0$, respectively, in different regions of the (c, b)-parametric half-plane, we obtain the bifurcations of phase portraits of (11) shown in Figs. 1(a)–1(d) and Figs. 2(a)–2(f), respectively.

(ii) $k_1 \neq 0$, $k_2 \equiv 0$.

In this case, $A = \frac{2(b+c)}{k_1}$, $\Delta = -32k_1(b+c)$, $\Delta_1 = 8k_1b^2$, $R = -\frac{2c}{k_1}$, $\varphi_0 = 0$, $\varphi_1 = -\frac{\sqrt{-2k_1(b+c)}}{k_1} = -\varphi_2$, $\varphi_s = 0$, $Y_\pm = \pm\sqrt{\frac{2c}{k_1}}$, $h_0 = 0$, $h_1 = \frac{(b+c)^2}{k_1^2} = h_2$, $h_s = \frac{c^2}{k_1^2}$.

Equation (8) has the form

$$\frac{d\varphi}{d\eta} = -y\left(\frac{2c}{k_1} - \varphi^2 + y^2\right), \quad \frac{dy}{d\eta} = \varphi\left(\frac{2(b+c)}{k_1} + \varphi^2 - y^2\right). \tag{12}$$

For $k_1 > 0$ and $k_1 < 0$, respectively, in different regions of the (c, b)-parametric half-plane, we obtain the bifurcations of phase portraits of (12) shown in Figs. 3(a)–3(h) and Figs. 4(a)–4(f), respectively.

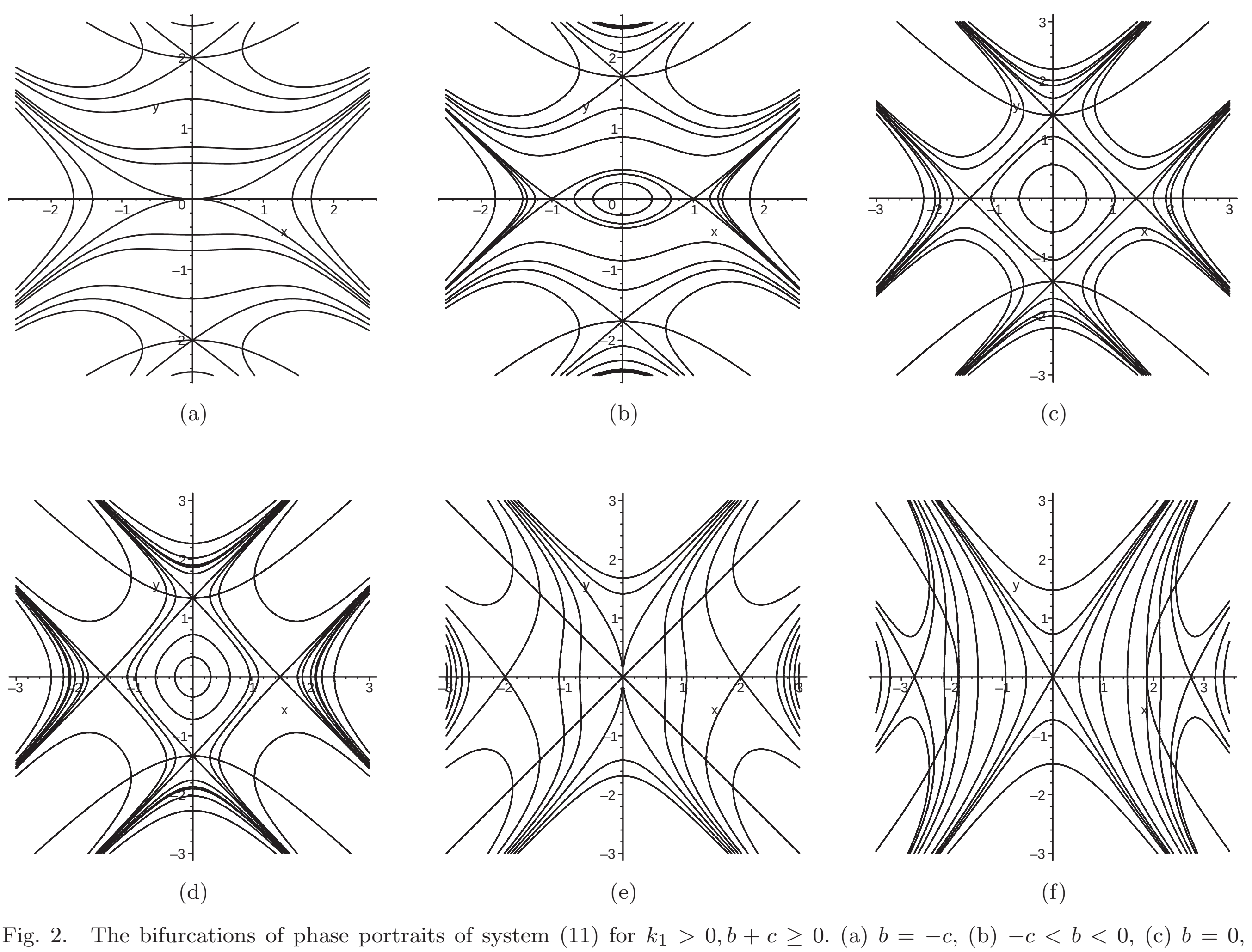

Fig. 2. The bifurcations of phase portraits of system (11) for $k_1 > 0, b + c \geq 0$. (a) $b = -c$, (b) $-c < b < 0$, (c) $b = 0$, (d) $0 < b < c$, (e) $b = c$ and (f) $c < b < \infty$.

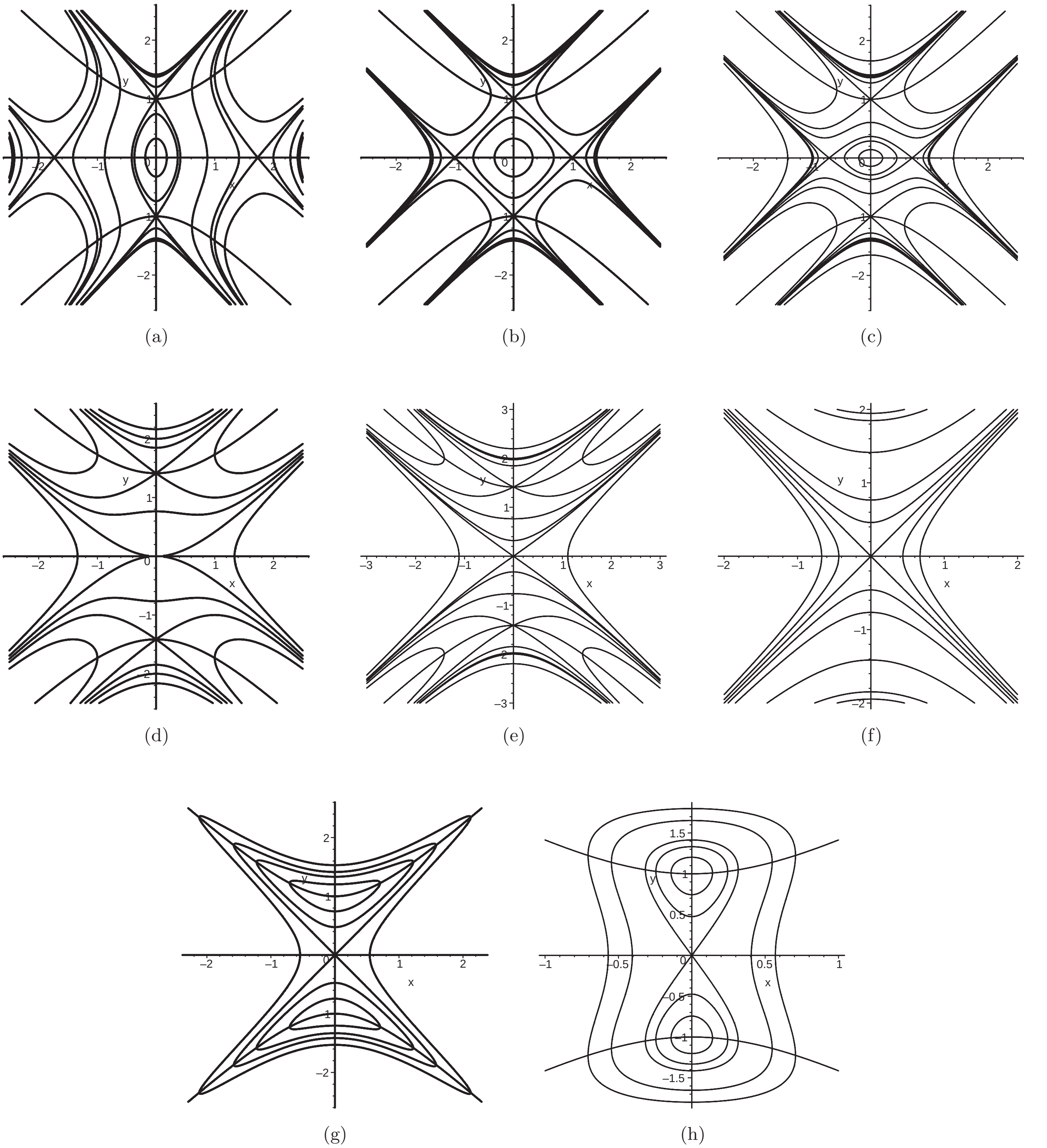

Fig. 3. The bifurcations of phase portraits of system (12) for $k_1 > 0, k_2 \equiv 0$. (a) $-\infty < b < -2c$, (b) $b = -2c$, (c) $-2c < b < c$, (d) $b = -c$, (e) $-c < b < 0$, (f) $b = 0$, (g) $0 < b < c$ and (h) $b \geq c$.

2. ***The case of*** $\boldsymbol{B \neq 0}$**.** In this case, the vector fields defined by (8) are nonsymmetric.

Suppose that $b + c < 0, k_1 \neq 0$, for a fixed $c > 0$. In this case, corresponding to the different parameter regions in the (k_1, k_2)-plane partitioned by the following bifurcation curves:

$$k_1 = 0, \quad k_2 = 0, \quad k_2^2 = 4bk_1,$$

$$k_2^2 = \frac{32(b+c)}{9}k_1 \equiv \lambda_1 k_1, \quad k_2^2 = \frac{8b^2}{2b-c}k_1 \equiv \lambda_2 k_1,$$

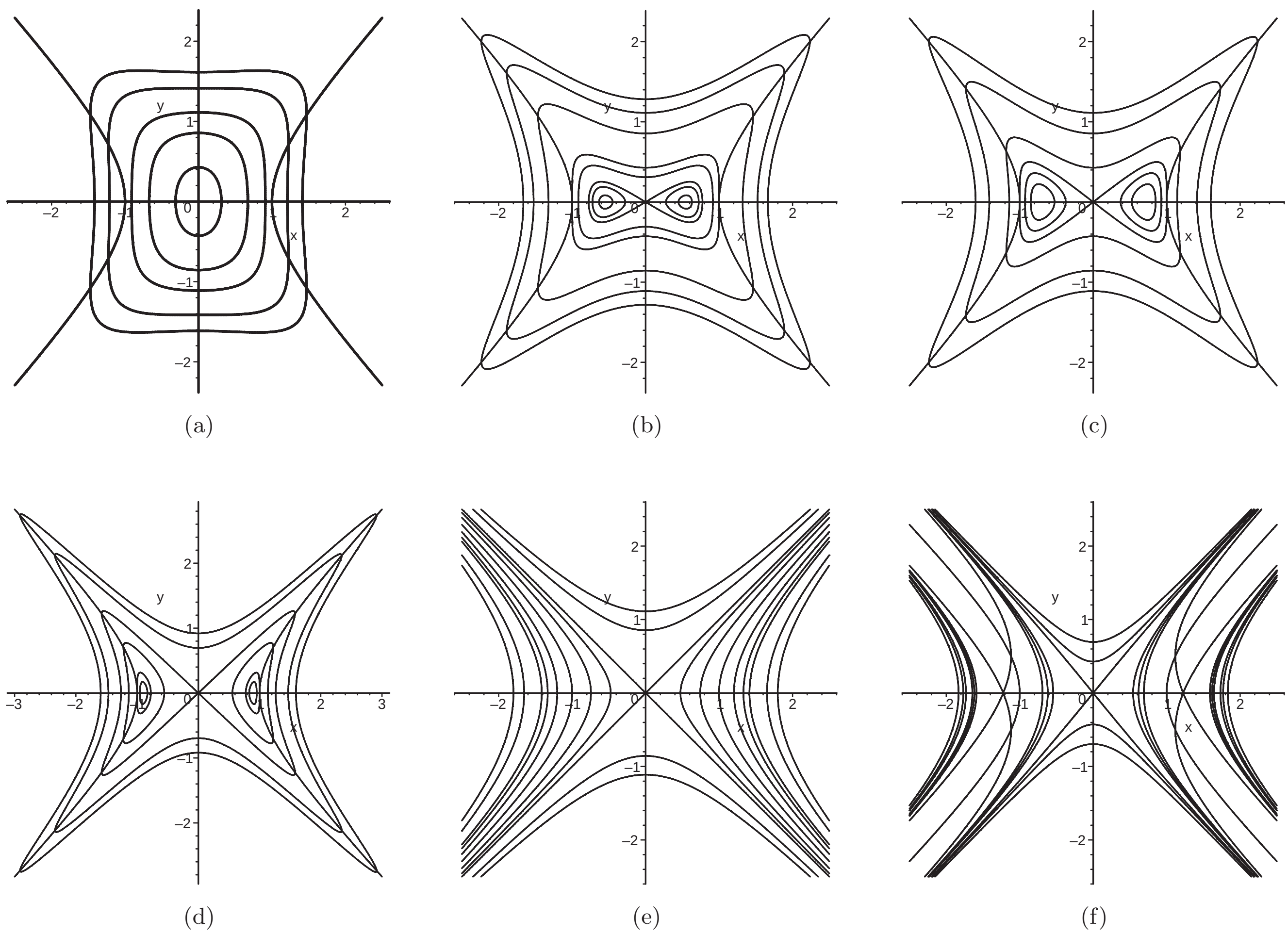

Fig. 4. The bifurcations of phase portraits of system (12) for $k_1 < 0, k_2 \equiv 0$. (a) $-\infty < b \le -c$, (b) $-c < b < -\frac{1}{2}c$, (c) $b = -\frac{1}{2}c$, (d) $-\frac{1}{2}c < b < 0$, (e) $b = 0$ and (f) $b > 0$.

we have the phase portraits of (8) shown in Fig. 5(a)–5(v).

Similarly, for $c > 0, b + c < 0$ and $-c < b \le 0$, $0 < b \le 2c$, $b > 2c$, respectively, we can obtain similar bifurcations of phase portraits of (8). To save space, we omit them.

As in [Li *et al.*, 2010], system (7) is called the associated regular system of (5). Unlike the first class of singular traveling system (see [Li & Chen, 2007; Li & Dai, 2007]), for the second class of singular traveling wave systems determined by Eq. (5) (or ($5_{\rm a}$)), even its associated regular system (7) (or (8)) has a family of smooth periodic solutions and homoclinic or heteroclinic orbits, the existence of singular curves defined by $\varphi^2 - y^2 = R$ implies the existence of breaking wave solutions $\varphi(\xi)$ of Eq. (3), when the phase orbits of these solutions intersect with a branch of the singular curve $\varphi^2 - y^2 = R$ at two points. Note that the two branches of hyperbola $\varphi^2 - y^2 = R$ are two singular curves of the vector field defined by system ($5_{\rm a}$). For example, consider the case of $\varphi > 0$ in Fig. 1(a), when ξ is varied along the loop orbit defined by $H(\phi, y) = h_2 = 0$ and passes through the hyperbola, on both the left-hand and the right-hand sides of the hyperbola $\varphi^2 - y^2 = R$, the vector field defined by system ($5_{\rm a}$) has opposite directions. This implies that the loop orbit of system ($5_{\rm a}$), defined by $H_1(\phi, y) = h_2$, consists of three breaking wave solutions of Eq. (2).

Similarly, for a closed orbit defined by $H_1(\phi, y) = h$ with $|h - h_2| \ll 0$, if it intersects the hyperbola $\phi - y^2 = R$ at two points then this closed orbit consists of three breaking wave solutions of Eq. (2).

Generally, for the first class of singular traveling wave systems, near a singular straight line $\phi = \phi_s$, ξ is a "slow time scale" variable while η is a "fast time scale" variable. But, for the second class of singular traveling wave systems, we know that both ξ and η have the same "time scale".

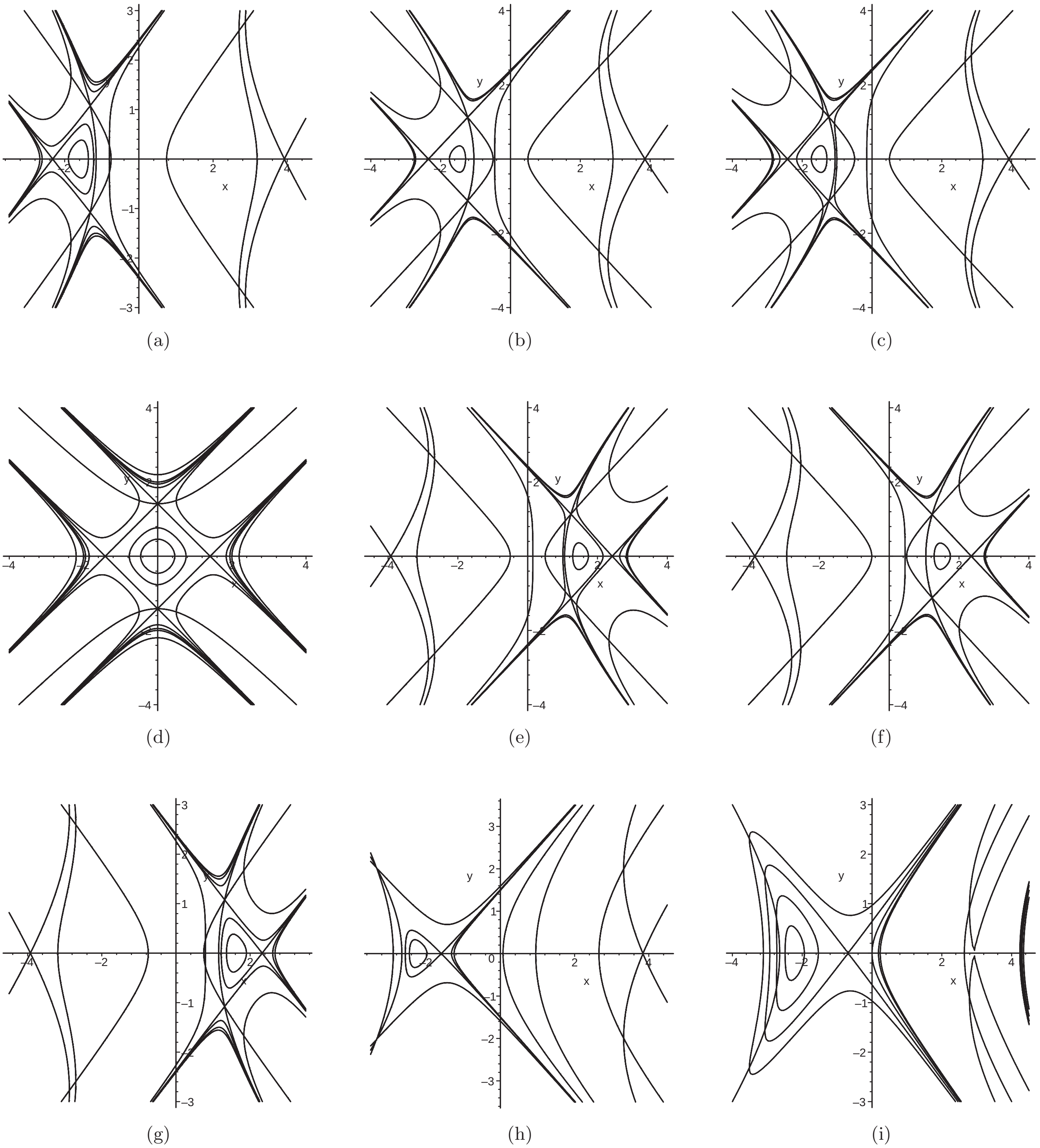

Fig. 5. The bifurcations of phase portraits of system (8) for $b + c < 0$. (a) $k_1 > 0$, $k_2 < 0$, $h_0 < h_1 < h_s$, (b) $k_1 > 0$, $k_2 < 0$, $h_0 < h_1 = h_s$, (c) $k_1 > 0$, $k_2 < 0$, $h_0 < h_s < h_1$, (d) $k_1 > 0$, $k_2 = 0$, $h_0 < h_1 = h_2 = h_s$, (e) $k_1 > 0$, $k_2 > 0$, $h_0 < h_s < h_2$, (f) $k_1 > 0$, $k_2 > 0$, $h_0 < h_s = h_2$, (g) $k_1 > 0$, $k_2 > 0$, $h_0 < h_2 < h_s$, (h) $k_1 < 0$, $k_2 > \sqrt{4bk_1}$, (i) $k_1 < 0$, $k_2 = \sqrt{4bk_1}$, (j) $k_1 < 0$, $\sqrt{\lambda_2 k_1} < k_2 < \sqrt{4bk_1}$, (k) $k_1 < 0$, $k_2 = \sqrt{\lambda_2 k_1}$, (l) $k_1 < 0$, $\sqrt{\lambda_1 k_1} < k_2 < \sqrt{\lambda_2 k_1}$, (m) $k_1 < 0$, $k_2 = \sqrt{\lambda_1 k_1}$, (n) $k_1 < 0$, $0 < k_2 < \sqrt{\lambda_1 k_1}$, (o) $k_1 < 0$, $k_2 = 0$, (p) $k_1 < 0$, $0 > k_2 > -\sqrt{\lambda_1 k_1}$, (q) $k_1 < 0$, $k_2 = -\sqrt{\lambda_1 k_1}$, (r) $k_1 < 0$, $-\sqrt{\lambda_1 k_1} > k_2 > -\sqrt{\lambda_2 k_1}$, (s) $k_1 < 0$, $k_2 = -\sqrt{\lambda_2 k_1}$, (t) $k_1 < 0$, $-\sqrt{\lambda_2 k_1} > k_2 > -\sqrt{4bk_1}$, (u) $k_1 < 0$, $k_2 = -\sqrt{4bk_1}$ and (v) $k_1 < 0$, $k_2 < -\sqrt{4bk_1}$.

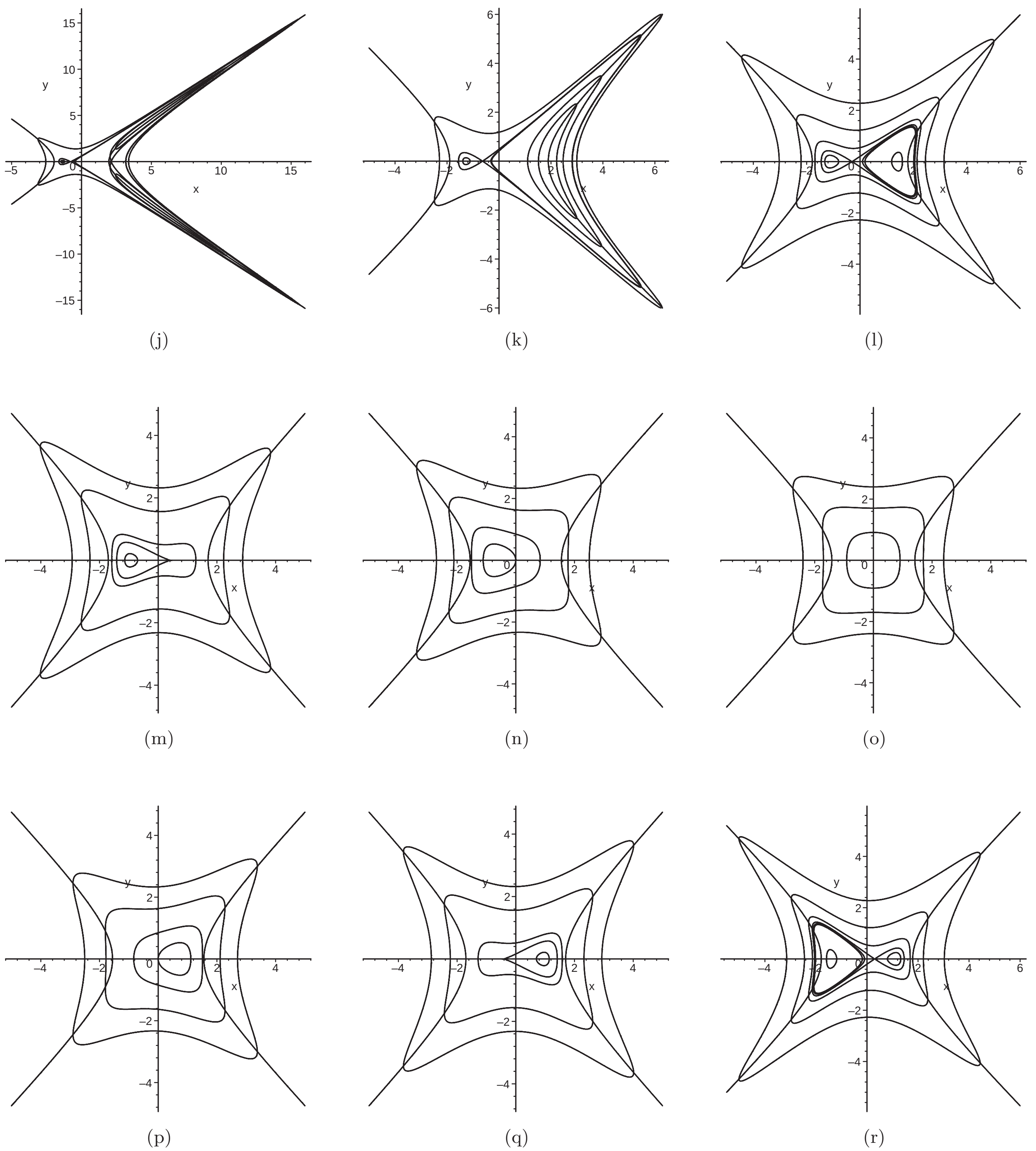

Fig. 5. (*Continued*)

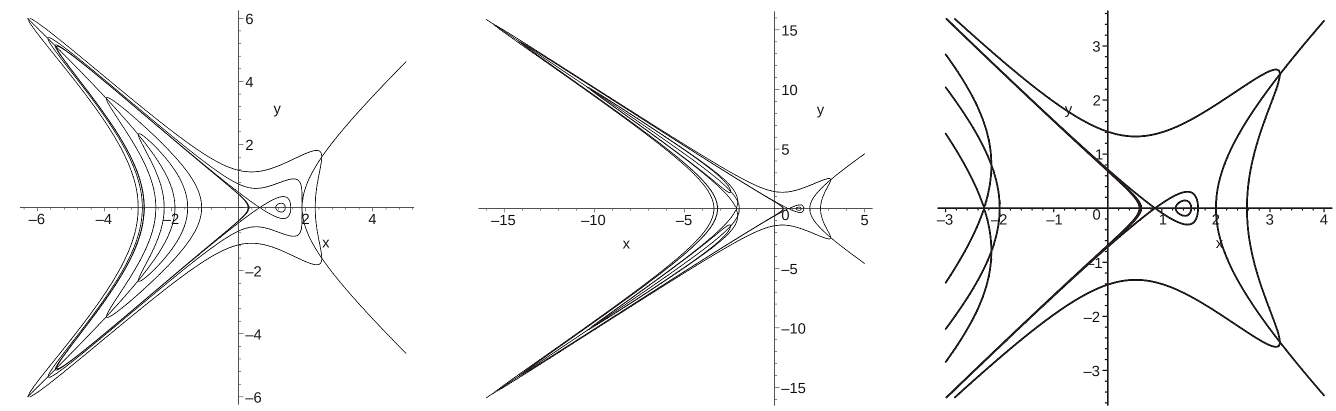

(s) (t) (u)

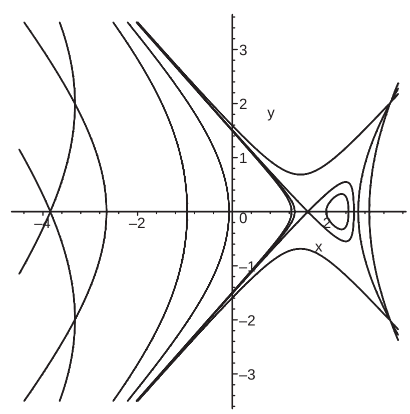

(v)

Fig. 5. (*Continued*)

3. Some Exact Traveling Wave Solutions of (1) in the Symmetric Case

To investigate the exact parametric representations of the traveling wave solutions of Eq. (2), we first consider system (8) with $B = 0$. By using the polar coordinates $\varphi = r\cos\theta, y = r\sin\theta$, system (8) becomes

$$\frac{dr}{d\eta} = r\sin 2\theta\left(r^2\cos 2\theta + \frac{1}{2}A\right), \quad \frac{d\theta}{d\eta} = r^2\cos^2 2\theta + A\cos^2\theta + R\sin^2\theta, \tag{13}$$

which has the first integral

$$r^4\cos^2 2\theta + 2r^2(A\cos^2\theta + R\sin^2\theta) + 4h = 0. \tag{14}$$

By using (14), we obtain

$$\begin{aligned}\frac{d\theta}{d\eta} &= \pm\frac{1}{2}\sqrt{((A-R)^2 - 16h)\cos^2 2\theta + 2(A^2 - R^2)\cos 2\theta + (A+R)^2} \\ &\equiv \pm\sqrt{V(\theta, h)}\end{aligned} \tag{15}$$

and

$$d\xi = (\varphi^2 - y^2 - R)d\eta = (r^2\cos 2\theta - R)d\eta. \tag{16}$$

3.1. *M-shape and W-shape wave profiles consisting of three breaking waves*

Suppose that $k_1 < 0, k_2^2 = 4k_1(b+c) > 0, b+c < 0$. We discuss the homoclinic orbits defined by $H_1(\varphi, y) = 0$ to the origin $O(0,0)$ shown in Figs. 1(a)–1(c). We see from (15) that $\tan\theta = \sqrt{\frac{b+c}{b-c}}\tanh(\omega_1\eta)$, where $\omega_1 = \frac{1}{2|k_1|}\sqrt{b^2-c^2}$. Thus, we have the solutions of (13) as follows:

$$\varphi(\eta) = \pm\frac{(b-c)\sqrt{\dfrac{2(b+c)}{k_1}}\cosh(\omega_1\eta)}{(b+c)-2c\cosh^2(\omega_1\eta)}. \quad (17)$$

To have the parametric representations of the traveling wave solutions of (1) with respect to ξ, we see from (13) that

$$d\xi = \frac{2d\theta}{\cos 2\theta} + \frac{(b-c)d\theta}{(b+c)\cos^2\theta + (b-c)\sin^2\theta}. \quad (18)$$

It implies that corresponding to two homoclinic orbits, Eq. (2) has the M-shape and W-shape wave profiles:

$$\varphi(\chi) = \pm\frac{(b-c)\sqrt{\dfrac{2(b+c)}{k_1}}\cosh(\chi)}{(b+c)-2c\cosh^2(\chi)},$$

$$\xi(\chi) = -\frac{1}{2}\sqrt{\frac{b-c}{b+c}}\chi - \ln\left(\frac{1+\sqrt{\dfrac{b+c}{b-c}}\tanh(\chi)}{1-\sqrt{\dfrac{b+c}{b-c}}\tanh(\chi)}\right). \quad (19)$$

When $-\infty < b < -3c$, corresponding to two homoclinic orbits, the functions defined by (17) and (19) give rise to M-shape and W-shape wave profiles of Eq. (2) consisting of three breaking waves as shown in Fig. 6(a) and 6(b), respectively. When $-3c \le b < -c$, the functions defined by (17) and (19) give rise to the solitary waves shown in Figs. 6(c) and 6(d), respectively.

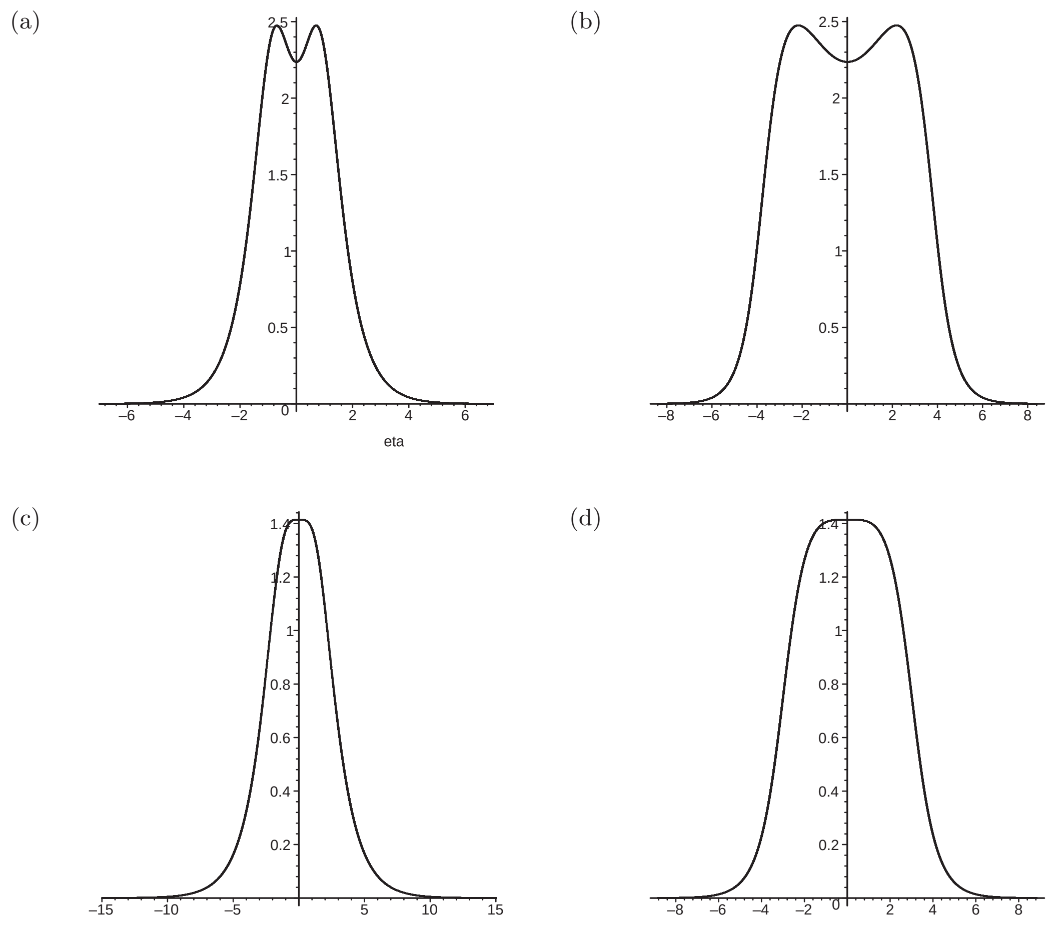

Fig. 6. The profiles of waves with respect to η and ξ, respectively. (a) $\varphi(\eta)$, (b) $\varphi(\xi)$, (c) $\varphi(\eta)$ and (d) $\varphi(\xi)$.

3.2. *Smooth kink and anti-kink waves*

3.2.1. *Suppose that* $k_1 > 0,\ k_2^2 = 4k_1(b+c) > 0,\ b+c > 0,\ b < 0,\ c > 0$

We discuss two heteroclinic orbits defined by $H_1(\varphi, y) = h_1 = \frac{(b+c)^2}{4k_1^2}$ connecting two equilibrium points $E_1(\varphi_1, 0)$ and $E_0(\varphi_0, 0)$ as shown in Fig. 2(b). We can see from (15) that $\tan\theta = \alpha_2 \tanh(\omega_2\eta)$, Thus, we have the solutions of (13) as follows:

$$\varphi(\eta) = \pm\frac{\sqrt{|b|(b+c)}\sinh(\omega_2\eta)}{(\sqrt{c} + \sqrt{|b|}\cosh(\omega_2\eta)}, \tag{20}$$

where $\alpha_2 = \sqrt{\frac{|b|}{b+c}}, \omega_2 = \frac{2}{k_1}\sqrt{c(b+c)}$.

To have the parametric representations of the traveling wave solutions of Eq. (2) with respect to ξ, we obtain from (14) that

$$d\xi = \frac{1}{k_1}\left[-\frac{1}{2\cos 2\theta} + \frac{2c}{\cos 2\theta\sqrt{V(\theta, h_1)}} + \frac{2c}{\sqrt{V(\theta, h_1)}}\right] d\theta, \tag{21}$$

where $V(\theta, h_1) = \frac{1}{k_1^2}[-(c(2b+c)\cos^2 2\theta + 2bc\cos 2\theta + c^2]$. It shows that, corresponding to two heteroclinic orbits, Eq. (2) has a kink wave solution and an anti-kink wave solution:

$$\begin{aligned} \varphi(\chi) &= \pm\frac{\sqrt{|b|(b+c)}\sinh(\chi)}{(\sqrt{c} + \sqrt{|b|}\cosh(\chi)}, \\ \xi(\chi) &= 2c\chi - \frac{1}{4k_1}\ln\frac{1+2w+w^2}{1-2w+w^2} + \sqrt{c(c+b)}\ln\frac{(w+1)(\alpha_2^2 + w + \alpha_2\sqrt{1+\alpha_2^2}\cosh\chi)}{(w-1)(\alpha_2^2 - w + \alpha_2\sqrt{1+\alpha_2^2}\cosh\chi)}, \end{aligned} \tag{22}$$

where $w = \alpha_2 \sinh(\chi)$.

3.2.2. *Suppose that* $k_1 > 0$,
$k_2^2 = 4k_1(b+c) > 0,\ b = 0$

We discuss four heteroclinic orbits defined by $H_1(\varphi, y) = h_1 = h_0 = \frac{c^2}{4k_1^2}$ connecting four equilibrium points $E_1(\varphi_1, 0)$, $S_{1,2}(0, Y_\pm)$ and $E_0(\varphi_0, 0)$ as shown in Fig. 2(c). We obtain from (15) that $\frac{d\theta}{d\eta} = \frac{c}{k_1}\sin(2\theta)$. Thus, for the heteroclinic orbit S_+E_0 connecting $S_1(0, Y_+)$ and $E_0(\varphi_0, 0)$, we have the following parametric representation with respect to η:

$$\varphi(\eta) = \frac{\sqrt{\frac{c}{k_1}}}{1 + e^{-\frac{2c}{k_1}\eta}}. \tag{23}$$

Noting that $d\xi = (\frac{1}{\sin 2\theta} + \frac{2}{\sin 4\theta} - \frac{1}{\cos 2\theta})d\theta$, we have a kink wave solution of Eq. (2) as follows:

$$\begin{aligned} \varphi(\chi) &= \frac{\sqrt{\frac{c}{k_1}}}{1 + e^{-\chi}}, \\ \xi(\chi) &= \frac{1}{2}(\chi + \ln\cosh\chi). \end{aligned} \tag{24}$$

For the heteroclinic orbit S_-E_0 connecting $S_2(0, Y_-)$ and $E_0(\varphi_0, 0)$, we obtain an anti-kink wave solution of Eq. (2) with the parametric representation with respect to ξ:

$$\varphi(\chi) = \frac{\sqrt{\frac{c}{k_1}}}{1 + e^{-\chi}}, \quad \xi(\chi) = -\frac{1}{2}(\chi + \ln\cosh\chi). \tag{25}$$

4. Smooth Solitary Waves

Suppose that $k_1 > 0, k_2^2 = 4k_1(b+c) > 0, 0 < b < c$. We discuss two heteroclinic orbits defined by $H_1(\varphi, y) = h_s = \frac{(b-c)^2}{4k_1^2}$ connecting two equilibrium points $S_{1,2}(0, Y_\pm)$ shown in Fig. 2(d). We obtain from (13) that $\tan\theta = \sqrt{\frac{b}{c-b}}\sinh(\omega_3\eta) \equiv \alpha_3\sinh(\omega_3\eta)$, where $\omega_3 = \frac{2}{k_1}\sqrt{c(c-b)}$. Thus, we have the solutions of (11) as follows:

$$\phi(\eta) = \pm\frac{c-b}{\sqrt{c} + \sqrt{b}\cosh(\omega_3\eta)}. \tag{26}$$

To have the parametric representations of the traveling wave solutions of Eq. (2) with respect

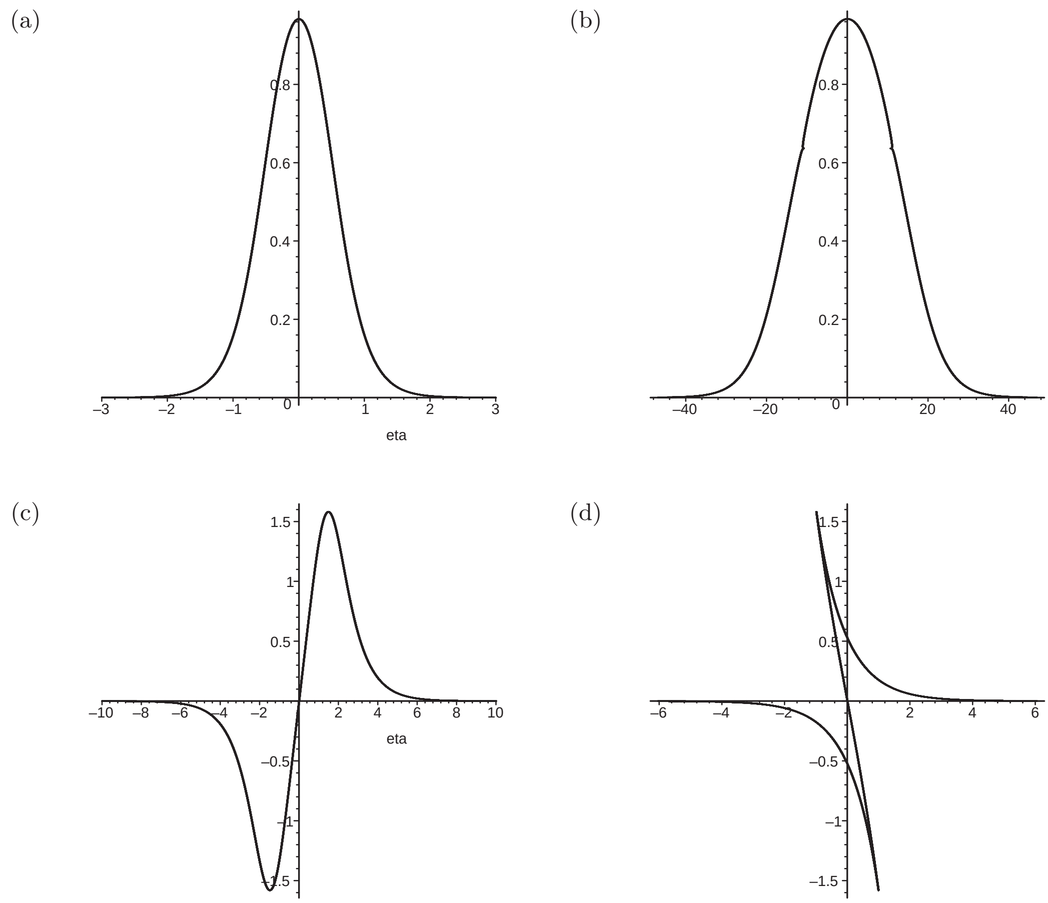

Fig. 7. The profiles of waves with respect to η and ξ, respectively. (a) $\varphi(\eta)$, (b) $\varphi(\xi)$, (c) $\varphi(\eta)$ and (d) $\varphi(\xi)$.

to ξ, we get from (14) that

$$d\xi = \frac{1}{k_1}\left[-\frac{1}{2\cos 2\theta} + \frac{2c}{\cos 2\theta\sqrt{V(\theta,h_s)}} + \frac{2c}{\sqrt{V(\theta,h_s)}}\right]d\theta, \tag{27}$$

where $V(\theta,h_s) = \frac{1}{k_1^2}[c(2b-c)\cos^2 2\theta + 2bc\cos 2\theta + c^2]$. It implies that, corresponding to two heteroclinic orbits, Eq. (2) has two solitary wave solutions:

$$\varphi(\chi) = \pm\frac{c-b}{\sqrt{c}+\sqrt{b}\cosh(\chi)},$$
$$\xi(\chi) = 2c\chi - \frac{1}{4k_1}\ln\frac{1+2w+w^2}{1-2w+w^2} + \sqrt{c(c-b)} \times \ln\frac{(w+1)(\alpha_3^2+w+\alpha_3\sqrt{1+\alpha_3^2}\cosh\chi)}{(w-1)(\alpha_3^2-w+\alpha_3\sqrt{1+\alpha_3^2}\cosh\chi)}, \tag{28}$$

where $w = \alpha_3\sinh(\chi)$.

Corresponding to two heteroclinic orbits as shown in Fig. 2(d), the functions defined by (26) and (28) give rise to two solitary wave solutions which are shown in Figs. 7(a) and 7(b), respectively.

5. Two-Peak Wave Profiles Consisting of Three Breaking Waves

Suppose that $k_1 > 0$, $k_2 = 0$, $0 < b < c$ or $b \geq c > 0$. We discuss the homoclinic orbits defined by $H_1(\varphi, y) = 0$ to the origin $O(0,0)$ shown in Figs. 3(g) and 3(h). We obtain from (13) that $\tan\theta = \alpha_4\tanh(\omega_4\eta)$, where $\alpha_4 = \sqrt{\frac{c}{b+c}}$, $\omega_4 = \frac{2}{k_1}\sqrt{c(b+c)}$. Thus, we have the solutions of (12) as follows:

$$\varphi(\eta) = \pm\frac{c\sqrt{2(b+c)}\sinh(\omega_4\eta)}{c+b\cosh^2(\omega_4\eta)}. \tag{29}$$

To have the parametric representations of the traveling wave solutions of Eq. (2) with respect to ξ, we get from (13) that

$$d\xi = \frac{2d\theta}{\cos 2\theta} + \frac{c\,d\theta}{(b+c)\cos^2\theta - c\sin^2\theta}. \quad (30)$$

It means that, corresponding to two homoclinic orbits, Eq. (2) has a two-peak wave solution:

$$\varphi(\chi) = \pm\frac{c\sqrt{2(b+c)}\sinh(\chi)}{c + b\cosh^2(\chi)},$$

$$\xi(\chi) = -\frac{1}{2}\sqrt{\frac{c}{b+c}}\chi - \ln\left(\frac{1+\sqrt{\frac{b+c}{c}}\tanh(\chi)}{1-\sqrt{\frac{b+c}{c}}\tanh(\chi)}\right). \quad (31)$$

Corresponding to two homoclinic orbits in Fig. 3(h), the functions defined by (31) give rise to two-peak wave profiles of Eq. (2) consisting of three breaking waves shown in Fig. 7(d).

6. The Exact Traveling Wave Solutions of Eq. (2) in a Nonsymmetric Case

Now, assume that $B \neq 0$. We know from (10) that in order to obtain exact solutions of (8), we must assume that $A = -R$, i.e. the conditions $k_2 = \pm\sqrt{4k_1 b}, A = \frac{2c-b}{k_1} = -R, \Delta = 4k_1(b-8c), B = \frac{(-2c)\sqrt{k_1 b}}{k_1^2}$ are satisfied.

Suppose that (i) $k_2 = -\sqrt{4k_1 b}$, $b > 8c > 0$, $k_1 > 0$ or (ii) $k_2 = \sqrt{4k_1 b}$, $b < 0$, $k_1 < 0$. Then, there exist three equilibrium points of (8): $E_0(\varphi_0, 0)$, $E_{1,2}(\varphi_{1,2}, 0)$, where $\varphi_0 = \mp\sqrt{\frac{b}{k_1}}$, $\varphi_{1,2} = \pm\frac{1}{2\sqrt{|k_1|}}[\sqrt{|b|} \mp \sqrt{|b-8c|}]$.

Thus, under the parametric conditions (i), we have the phase portrait of (8) as shown in Figs. 8(a)–8(c), where the parameter value is $b = b_M$ such that $\varphi_M = \sqrt{R}$ and $(\varphi_M, 0)$ is the intersection point of the homoclinic orbit to the equilibrium $(\varphi_1, 0)$ with the φ-axis.

Under the parametric conditions (ii), we have the phase portrait of (8) as shown in Figs. 9(a)–9(c), where the parameter value is $b = b_m$ such that $\varphi_m = -\sqrt{R}$ and $(\varphi_m, 0)$ is the intersection point of the homoclinic orbit to the equilibrium $(\varphi_1, 0)$ with the φ-axis.

To find the parametric representations of the homoclinic orbits shown in Fig. 8, we first obtain from (10) that

$$y^2 = (\varphi^2 - R) \pm \sqrt{(R^2 - 4h) - 4B\varphi}. \quad (32)$$

On the left-hand side of the positive half-branch of the hyperbola $\varphi^2 - y^2 = R$, along the loop orbit (a branch of the level curve of $H_1(\phi, y) = h$), we have $y^2 = (\varphi^2 - R) + \sqrt{(R^2 - 4h) - 4B\varphi}$; while on the right-hand side, $y^2 = (\varphi^2 - R) - \sqrt{(R^2 - 4h) - 4B\varphi}$.

When $y = 0$, (32) becomes

$$\varphi^4 - 2R\varphi^2 + 4B\varphi + 4h = 0.$$

For $h = h_1 = H_1(\varphi_1, 0)$, we have

$$\varphi^4 - 2R\varphi^2 + 4B\varphi + 4h_1 = (\varphi - \varphi_1)^2(\varphi - \varphi_M)(\varphi - \varphi_3)$$

with $\varphi_3 < \varphi_1 < \varphi_2 < \varphi_M$.

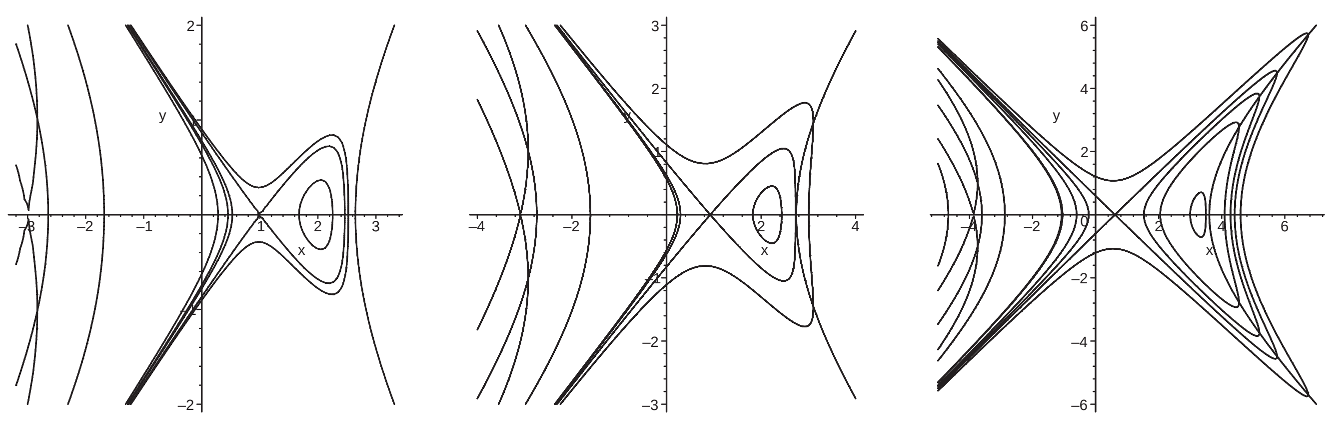

(a) (b) (c)

Fig. 8. The phase portraits of (8) when $B \neq 0, k_1 > 0, b > 8c > 0$. (a) $8c < b < b_M$, (b) $b = b_M$ and (c) $-\infty < b < b_M$.

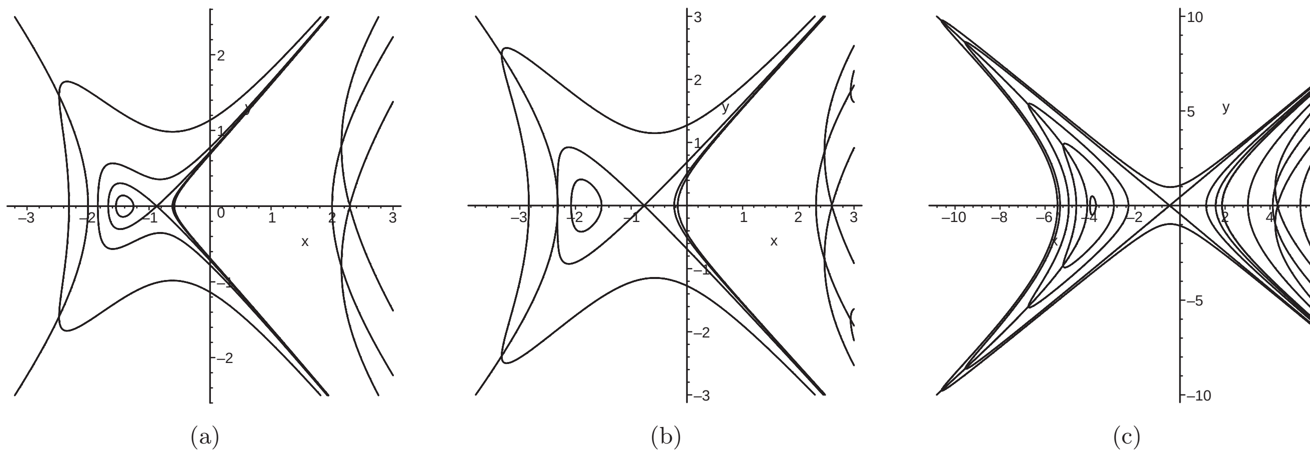

Fig. 9. The phase portraits of (8) when $B \neq 0, k_1 < 0, b < 0$. (a) $b_m < b < 0$, (b) $b = b_m$ and (c) $-\infty < b < b_m$.

Let $\psi^2 = (R^2 - 4h) - 4B\varphi$, i.e. $\varphi = \frac{1}{4B}(R^2 - 4h - \psi^2)$. Then, (32) becomes

$$\begin{aligned} y^2 &= \frac{1}{16B^2}[(R^2-4h)^2 - 16B^2R \pm 16B^2\psi \\ &\quad - 2(R^2-4h)\psi^2 + \psi^4] \\ &\equiv \frac{1}{16B^2}F_{1,2}(\psi). \end{aligned} \tag{33}$$

Thus, we have

$$\begin{aligned} \frac{d\psi}{d\eta} &= \pm\frac{1}{2}\sqrt{F_{1,2}(\psi)}, \\ \frac{d\psi}{d\xi} &= \pm\frac{1}{2\psi}\sqrt{F_{1,2}(\psi)}. \end{aligned} \tag{34}$$

Considering the homoclinic orbit defined by $H_1(\varphi, y) = h_1$ in Fig. 8(c), the functions $F_{1,2}(\psi)$ on the right-hand side of Eq. (34) can be written as

$$\begin{aligned} F_1(\psi) &= \psi^4 + (8h_1 - 2R^2)\psi^2 + 16B^2\psi \\ &\quad + (R^4 - 16RB^2 - 8R^2h_1 + 16h_1) \\ &= (\psi - \psi_1)^2(\psi - \psi_3)(\psi - \psi_m), \end{aligned} \tag{35}$$

$$\begin{aligned} F_2(\psi) &= \psi^4 + (8h_1 - 2R^2)\psi^2 - 16B^2\psi \\ &\quad + (R^4 - 16RB^2 - 8R^2h_1 + 16h_1) \\ &= (\psi - \psi_a)^2(\psi - \psi_b)(\psi - \psi_M), \end{aligned} \tag{36}$$

where

$$\begin{aligned} \psi_1 &= \sqrt{(R^2-4h_1) - 4B\varphi_1}, \\ \psi_m &= -\sqrt{(R^2-4h_1) - 4B\varphi_M}, \\ \psi_3 &= -\sqrt{(R^2-4h_1) - 4B\varphi_3}, \\ \psi_3 &< \psi_m < \psi_1; \end{aligned}$$

$$\begin{aligned} \psi_a &= -\sqrt{(R^2-4h_1) - 4B\varphi_1}, \\ \psi_M &= \sqrt{(R^2-4h_1) - 4B\varphi_M}, \\ \psi_b &= \sqrt{(R^2-4h_1) - 4B\varphi_3}, \\ \psi_a &< \psi_M < \psi_b. \end{aligned}$$

It follows from the first equation of (34)–(36) that

$$\begin{aligned} \psi(\eta) &= \psi_1 \\ &\quad - \frac{2(\psi_1-\psi_3)(\psi_1-\psi_m)}{(\psi_m-\psi_3)\cosh(\omega_{01}\eta) + (2\psi_1-\psi_3-\psi_m)}, \\ &\quad \eta \in (-\infty, -Z_{h_1}) \cup \eta \in (Z_{h_1}, \infty); \end{aligned} \tag{37}$$

$$\begin{aligned} \psi(\eta) &= \psi_a \\ &\quad - \frac{2(\psi_a-\psi_b)(\psi_a-\psi_M)}{(\psi_M-\psi_b)\cosh(\omega_{02}\eta) + (2\psi_a-\psi_b-\psi_M)}, \\ &\quad \eta \in (-Z_{h_1}, Z_{h_1}), \end{aligned} \tag{38}$$

where

$$\begin{aligned} \omega_{01} &= \frac{1}{2}\sqrt{(\psi_1-\psi_3)(\psi_1-\psi_m)}, \\ \omega_{02} &= \frac{1}{2}\sqrt{(\psi_a-\psi_b)(\psi_a-\psi_M)}, \end{aligned}$$

Z_{h_1} is the value of η satisfying $\psi(Z_{h_1}) = \sqrt{(R^2-4h_1) - 4B\varphi_s}$, and (φ_s, y_s) is the coordinate of the intersection point of the homoclinic orbit $H_1(\varphi, y) = h_1$ and the singular curve $\varphi^2 - y^2 = R$.

Thus, a parametric representation of the homoclinic orbit of system (8) has been obtained, with respect to η, as follows:

$$\varphi(\eta) = \frac{1}{4B}(R^2 - 4h_1 - \psi^2(\eta)), \tag{39}$$

where $\psi(\eta)$ is given by (37) and (38).

In order to obtain the exact solutions of (2) with respect to the variable $\xi = x - ct$, by using (35) and the second equation of system (34), and by introducing a parametric variable χ, we obtain

$$\begin{aligned} \psi(\chi) &= \psi_1 - \frac{2(\psi_1 - \psi_m)(\psi_1 - \psi_3)}{(\psi_m - \psi_3)\cosh(\omega_{01}\chi) - (2\psi_1 - \psi_m - \psi_3)}, \\ \xi(\chi) &= x - ct = -2\left[\psi_1\chi + \ln\left(\frac{2\sqrt{(\psi - \psi_m)(\psi - \psi_3)} + 2\psi - (\psi_m + \psi_3)}{\psi_m - \psi_3}\right)\right]. \end{aligned} \tag{40}$$

Next, define a value χ_b of χ by the relationship

$$\varphi(\chi_b) = \frac{1}{4B}(R^2 - 4h_1 - \psi^2(\chi_b)) \equiv \varphi_s, \tag{41}$$

where $\psi(\chi)$ is given by (40). Corresponding to χ_b, the second formula of (40) gives the value of $\xi_b = \xi(\chi_b)$.

Thus, for $\xi \in (-\infty, -\xi_b)$, i.e. $\chi \in (\chi_b, \infty)$, we have the following exact and explicit parametric representation of a breaking wave solution of Eq. (2):

$$\begin{aligned} \varphi(\chi) &= \frac{1}{4B}(R^2 - 4h_1 - \psi^2(\chi)), \\ \xi(\chi) &= x - ct = -2\left[\psi_1\chi + \ln\left(\frac{2\sqrt{(\psi - \psi_m)(\psi - \psi_3)} + 2\psi - (\psi_m + \psi_3)}{\psi_m - \psi_3}\right)\right]. \end{aligned} \tag{42}$$

Using (36) to integrate the second equation of system (34) yields

$$\begin{aligned} \psi(\chi) &= \psi_a - \frac{2(\psi_a - \psi_b)(\psi_a - \psi_M)}{(\psi_M - \psi_b)\cosh(\omega_{02}\chi) + (2\psi_a - \psi_b - \psi_M)}, \\ \xi(\chi) &= x - ct = -2\left[\psi_a\chi + \ln\left(\frac{2\sqrt{(\psi - \psi_M)(\psi - \psi_b)} + 2\psi - (\psi_M - \psi_b)}{\psi_M - \psi_b}\right)\right]. \end{aligned} \tag{43}$$

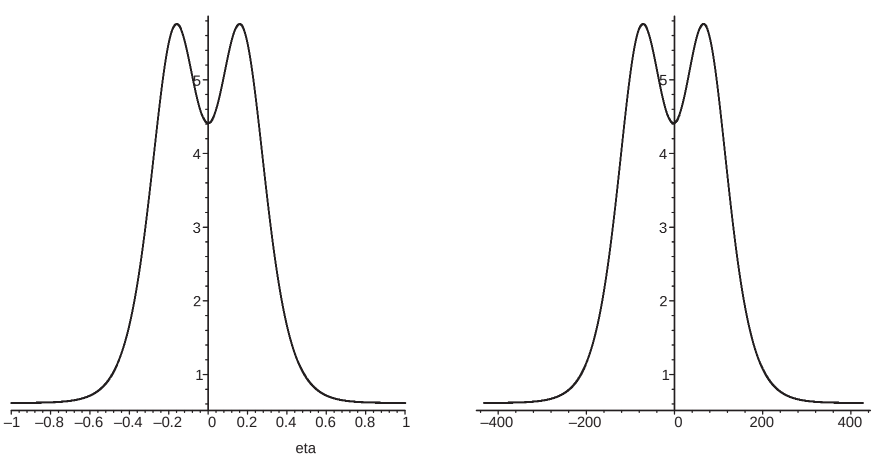

Fig. 10. The M-shape wave profiles with respect to η and ξ, respectively. (a) $\varphi(\eta)$ and (b) $\varphi(\xi)$.

Thus, for $\xi \in (\xi_b, \infty)$, i.e. $\chi \in (-\infty, -\chi_b)$, we have

$$\varphi(\chi) = \frac{1}{4B}(R^2 - 4h_1 - \psi^2(\chi)),$$
$$\xi(\chi) = x - ct = -2\left[\psi_a \chi + \ln\left(\frac{2\sqrt{(\psi - \psi_M)(\psi - \psi_b)} + 2\psi - (\psi_M - \psi_b)}{\psi_M - \psi_b}\right)\right], \tag{44}$$

which gives another breaking wave solution. For $\xi \in (0, \xi_b)$ and $\xi \in (-\xi_b, 0)$, systems (42) and (44) respectively determine the third exact breaking solutions. Figures 10(a) and 10(b) show the different wave profiles of the M-shape waves with respect to the variables η and ξ, respectively.

Similarly, by considering the phase orbits shown in Fig. 9, we can obtain the W-shape waves with respect to the variables η and ξ, respectively. In addition, corresponding to the homoclinic orbits shown in Figs. 8(a) and 8(b), formula (43) also gives rise to the exact parametric representation of the solitary wave solutions.

References

Camassa, R. & Holm, D. D. [1993] "An integrable shallow water equation with peaked solution," *Phys. Rev. Lett.* **71**, 1161–1164.

Camassa, R., Holm, D. D. & Hyman, J. M. [1994] "A new integrable shallow water equation," *Adv. Appl. Mech.* **31**, 1–33.

Constantin, A., Gerdjikov, V. S. & Ivanov, R. I. [2007] "Generalized Fourier transform for Cammasa–Holm hierarchy," *Inverse Probl.* **23**, 1565–1579.

Desanto, J. A. [1998] *Mathematical and Numerical Aspects of Wave Propagation* (SIAM, Philadelphia).

Fokas, A. S. [1995] "On a class of physically important integrable equations," *Physica D* **87**, 145–150.

Fuchssteiner, B. & Fokas, A. S. [1981] "Symplectic structures, their Bäcklund transformations and hereditary symmetries," *Physica D* **4**, 47–66.

Fuchssteiner, B. [1996] "Some tricks from symmetry-toolbox for nonlinear equations: Generalizations of the Camassa–Holm equation," *Physica D* **95**, 229–243.

Li, J., Wu, J. & Zhu, H. [2006] "Travelling waves for an integrable higher order KdV type wave equations," *Int. J. Bifurcation and Chaos* **16**, 2235–2260.

Li, J. & Chen, G. [2007] "On a class of singular nonlinear traveling wave equations," *Int. J. Bifurcation and Chaos* **17**, 4049–4065.

Li, J. & Dai, H. [2007] *On the Study of Singular Nonlinear Travelling Wave Equations: Dynamical Approach* (Science Press, Beijing).

Li, J. & Qiao, Z. [2010] "Bifurcations of traveling wave solutions for an integrable equation," *J. Math. Phys.* **51**, 042703.

Li, J., Zhao, X. & Chen, G. [2010] "On the breaking property for the second class of singular nonlinear traveling wave equations," *Int. J. Bifurcation and Chaos* **19**, 1289–1306.

Olver, P. J. & Rosenau, P. [1996] "Tri-Hamiltonian duality between solitons and solitary-wave solutions having compact support," *Phys. Rev. E* **53**, 1900–1906.

Qiao, Z. [2006] "A new integrable equation with cuspons and W/M-shape solitons," *J. Math. Phys.* **48**, 112701.

Qiao, Z. [2007] "New integrable hierarchy, its parametric solutions, cuspons, one-peak solutions, and M/W-shape solitons," *J. Math. Phys.* **49**, 082701.

Qiao, Z. & Li, X. [2011] "An integrable equation with nonsmooth solitons," *Theor. Math. Phys.* **167**, 584–589.